

# New Bounds on Axion-Like Particles From the Fermi Large Area Telescope observation of PKS 2155 – 304

Cun Zhang,<sup>1,2,3</sup> Yun-Feng Liang,<sup>2</sup> Shang Li,<sup>2</sup> Neng-Hui Liao,<sup>2</sup> Lei Feng,<sup>2,\*</sup> Qiang Yuan,<sup>2,†</sup> Yi-Zhong Fan,<sup>2,‡</sup> and Zhong-Zhou Ren<sup>1,3,§</sup>

<sup>1</sup>*School of Physics, Nanjing University, Nanjing, 210092, China*

<sup>2</sup>*Key Laboratory of Dark Matter and Space Astronomy,*

*Purple Mountain Observatory, Chinese Academy of Sciences, Nanjing 210008, China*

<sup>3</sup>*Joint Center for Particle, Nuclear Physics and Cosmology, Nanjing 210093, China*

## Abstract

The axion-like particle (ALP)-photon mixing in the magnetic field around  $\gamma$ -ray sources or along the line-of-sight could induce oscillation between photons and ALPs, which then causes irregularities in the  $\gamma$ -ray spectra. In this work we try to search for such spectral irregularities in the spectrum of PKS 2155 – 304 using 8.6 years of the Fermi Large Area Telescope (Fermi-LAT) data. No significant evidence for the presence of ALP-photon oscillation is obtained, and the parameter space of ALPs is constrained. The exclusion region sensitively depends on the poorly known magnetic field of host galaxy cluster of PKS 2155 – 304. If the magnetic field is as high as  $\sim 10 \mu\text{G}$ , the “hole”-like parameter region allowed in Ref. [1] can be ruled out.

PACS numbers: 14.80.Va, 95.85.Pw, 98.70.Rz

---

\*Electronic address: Corresponding author: fenglei@pmo.ac.cn

†Electronic address: Corresponding author: yuanq@pmo.ac.cn

‡Electronic address: Corresponding author: yzfan@pmo.ac.cn

§Electronic address: Corresponding author: zren@nju.edu.cn

## I. INTRODUCTION

As a generalization of the axion [2–6], the axion-like particle (ALP) is a very light pseudo-Goldstone boson predicted in several extensions of the Standard Model, such as the string theory [7, 8] and the Kaluza-Klein theory [9–11]. Thanks to its interaction with the electromagnetic field, an ALP could oscillate with a photon in an external electric or magnetic field, providing a promising way to detect it. Different from the axion, there is no relation between the ALP mass and its coupling strength which was employed to solve the Strong CP Problem [2].

ALPs belong to one kind of cold dark matter candidates known as weakly interacting slim particles (WISPs) [12–14]. Other than the search for the classical weakly interacting massive particles (WIMPs) dark matter [15–19], the detection of ALPs is usually based on the ALP-photon oscillation effect [20, 21, 23]. A high or large-scale electric or magnetic field is needed in such a kind of experiments. Several ground experiments, such as the Any Light Particle Search (ALPS) I [23] and the CERN Resonant WISP Search (CROWS) [24], have searched for such oscillation signals as the photon-ALP beam flying through the laboratory magnetic field. The CERN Axion Solar Telescope (CAST) and the proposed International Axion Observatory (IAXO) instead aim to detect the photons converted by solar axions (produced by the Primakoff effect as photons pass the Coulomb field of charged particles in the Sun) in the laboratory magnetic field. The relevant experimental progresses can be found in some recent review articles [25–28].

Magnetic field exists everywhere in the Universe. For some highly magnetized neutron stars (i.e., magnetars, [29]), the dipole magnetic fields could be high up to  $\geq 10^{14}$  G. There are also large-scale coherent magnetic fields in galaxies and galaxy clusters, with coherent lengths as long as tens of kpc. These high magnetic field objects or large-scale coherent regions are ideal targets to search for ALPs. Chelouche *et al.* [30] calculated the spectral signatures induced by ALP-photon oscillations in several astrophysical scenarios. The H.E.S.S. collaboration used the data of PKS 2155 – 304 to constrain the ALP parameter space [31]. The Fermi-LAT collaboration studied possible spectral irregularities in the  $\gamma$ -ray data of NGC 1275, and got strong constraints [1]. However, there is a “hole”-like region survived in their constraints [1]. In this work, we search for spectral irregularities using the Fermi-LAT data of PKS 2155 – 304. The uncertainties of the magnetic fields, including

both the distributions and the strengths, are discussed. With “optimistic” parameters, the “hole”-like region can be ruled out.

This work is organized as follows. In Section II, we briefly describe the ALP-photon oscillation model. In Section III, we discuss the magnetic field and electron distribution along the line-of-sight. In Section IV the analysis of the Fermi-LAT data of PKS 2155 – 304 to constrain the ALP parameters is given. The results are presented in Section V. Our conclusions are summarized in Section VI, together with some discussions.

## II. ALP-PHOTON OSCILLATION MODEL

The ALP-photon oscillation system can be described by the following Lagrangian [32]:

$$\mathcal{L} = -\frac{1}{4}F_{\mu\nu}F^{\mu\nu} + \frac{1}{2}(\partial_\mu a\partial^\mu a - m_a^2 a^2) - \frac{1}{4}g_{a\gamma}aF_{\mu\nu}\tilde{F}^{\mu\nu} + \frac{\alpha^2}{90m_e^4} \left[ (F_{\mu\nu}F^{\mu\nu})^2 + \frac{7}{4} (F_{\mu\nu}\tilde{F}^{\mu\nu})^2 \right] \quad (1)$$

where  $g_{a\gamma}$  is the coupling constant between ALPs and photons which has been found to be smaller than  $10^{-10} \text{ GeV}^{-1}$  for the ALP mass  $m_a \lesssim 1\mu\text{eV}$ . The last term is the Euler-Heisenberg-Weisskopf (EHW) effective Lagrangian [33] from the vacuum polarisation which is negligible as long as the magnetic field is much lower than the critical field strength  $B_c = m_e^2/e \approx 4.41 \times 10^{13} \text{ G}$ .

We describe the photon-ALP beam using the density matrix  $\rho(s)$  that is defined as

$$\rho(s) = \begin{pmatrix} A_1(s) \\ A_2(s) \\ a(s) \end{pmatrix} \otimes \begin{pmatrix} A_1(s) & A_2(s) & a(s) \end{pmatrix}^* , \quad (2)$$

where  $s$  is the position along the path of the photon-ALP beam in direction  $\mathbf{e}_3$ , and  $A_1, A_2$  are the photon transverse polarizations along axes  $\mathbf{e}_1, \mathbf{e}_2$ , respectively. In the short-wavelength limit where  $E \gg m_a$ , we get the Liouville-Von Neumann (LVN) equation

$$i\frac{d\rho(s)}{ds} = [\rho, \mathcal{M}] \quad (3)$$

with the mixing matrix  $\mathcal{M}$

$$\mathcal{M}_{\mathbf{B}_T \parallel \mathbf{e}_2} = \begin{pmatrix} \Delta_{pl} & 0 & 0 \\ 0 & \Delta_{pl} & \Delta_{a\gamma} \\ 0 & \Delta_{a\gamma} & \Delta_{aa} \end{pmatrix} , \quad (4)$$

where  $\mathbf{B}_T$  is the transversal magnetic field orientated along  $\mathbf{e}_2$ , and

$$\Delta_{a\gamma} = \frac{1}{2}g_{a\gamma}B_T \simeq 1.52 \times 10^{-2}g_{a\gamma,-11}B_{T,-6} \text{ kpc}^{-1}, \quad (5)$$

$$\Delta_{aa} = -\frac{m_a^2}{2E} \simeq -7.8 \times 10^{-2}m_{a,-9}^2E_9^{-1} \text{ kpc}^{-1}, \quad (6)$$

$$\Delta_{pl} = -\frac{w_{pl}^2}{2E} \simeq -1.1 \times 10^{-4}E_9^{-1} \left( \frac{n_e}{\text{cm}^{-3}} \right) \text{ kpc}^{-1}, \quad (7)$$

where  $w_{pl}$  is plasma frequency and  $n_e$  is the number density of free electrons,  $B_T = B_{T,-6}10^{-6}$  G,  $g_{a\gamma} = g_{a\gamma,-11}10^{-11} \text{ GeV}^{-1}$ ,  $m_a = m_{a,-9} \text{ neV}$ , and  $E = E_9 \text{ GeV}$ .

For a general magnetic field with angle  $\psi$  from  $\mathbf{e}_2$ , the mixing matrix becomes

$$\mathcal{M} = V\mathcal{M}_{\mathbf{B}_T \parallel \mathbf{e}_2}V^T, \quad (8)$$

with

$$V = \begin{pmatrix} \cos \psi & \sin \psi & 0 \\ -\sin \psi & \cos \psi & 0 \\ 0 & 0 & 1 \end{pmatrix}. \quad (9)$$

Finally, for an initial photon matrix  $\rho(s_0)$  at  $s_0$ , we can get the density matrix at position  $s$  by splitting the path to small regions where the magnetic field is approximately constant and homogeneous, as

$$\rho(s) = T(s, s_0)\rho(s_0)T^\dagger(s, s_0), \quad (10)$$

where  $T(s, s_0)$  is the transfer function defined as  $T(s, s_0) = \prod_0^n T(s_{i+1}, s_i)$ .

It is helpful to consider a simple case where the constant and homogeneous magnetic field satisfies  $\mathbf{B}_T \parallel \mathbf{e}_2$ . In this case, the conversion probability of an initially  $\mathbf{e}_2$  polarized photon to an ALP is

$$P_{a\gamma}(s, s_0) = \sin^2(2\theta) \sin^2 \left( \frac{\Delta_{\text{osc}}(s - s_0)}{2} \right), \quad (11)$$

where the mixing angle  $\theta$  and oscillation wave number  $\Delta_{\text{osc}}$  are

$$\theta = \frac{1}{2} \arctan \left( \frac{2\Delta_{a\gamma}}{\Delta_{pl} - \Delta_{aa}} \right), \quad (12)$$

$$\Delta_{\text{osc}} = [(\Delta_{pl} - \Delta_{aa})^2 + 4\Delta_{a\gamma}^2]^{1/2}. \quad (13)$$

In order to get a significant ALP-photon oscillation, the phases of the two sine functions should be large enough. Firstly the length of the propagation path  $l$  should be larger than

TABLE I: Parameters of the ICMF.

$\sigma_B$	$\Lambda_{\min}$	$\Lambda_{\max}$	$q$	$\eta$
3.0 $\mu\text{G}$	0.5 kpc	20 kpc	-11/3	0.5

the ALP-photon oscillation wave length  $l_{\text{osc}} = 4\pi/\Delta_{\text{osc}}$ . In a simple case where  $\Delta_{pl}$  and  $\Delta_{aa}$  are smaller than  $\Delta_{a\gamma}$ , we get  $l_{\text{osc}} = 2\pi/\Delta_{a\gamma}$ . Secondly, the energy should be higher than the lower critical energy  $E_L$  which reads

$$E_L = \frac{E(\Delta_{aa} - \Delta_{pl})}{2\Delta_{a\gamma}} \simeq \frac{2.5|m^2 - \omega_{pl}^2|}{(\text{neV})^2} B_{T,-6}^{-1} g_{a\gamma,-11}^{-1} \text{ GeV}. \quad (14)$$

### III. PHOTON TRAVEL ENVIRONMENTS

To get the survival probability of a  $\gamma$ -ray photon which travels from the source to the detector, we need to consider its propagation in four main regions: the source region (surrounding PKS 2155 – 304), the inter-cluster region, the extragalactic space, and the interior of the Milky Way.

In the source region, the magnetic field and electron density are  $B \approx 70 (r/\text{pc})^{-1.31} \mu\text{G}$  and  $n_e \approx 2 \times 10^4 (r/\text{pc})^{-1.35} \text{ cm}^{-3}$ , respectively [34]. With the ALP parameter range considered in this work (i.e.,  $10^{-12} \text{ GeV}^{-1} < g_{a\gamma} < 10^{-10} \text{ GeV}^{-1}$ ,  $10^{-1} \text{ neV} < m_a < 10^2 \text{ neV}$ ), the oscillation in the source region is negligible.

There are no observations about the inter-cluster magnetic fields (ICMFs) around PKS 2155 – 304. The typical magnetic field strength in galaxy clusters is in the range of 1 – 10  $\mu\text{G}$  [45]. Following Ref. [44], we describe the ICMFs as Gaussian turbulent fields with mean value zero and variance  $\sigma_B$ . The power spectrum follows a power-law  $M(k) \propto k^q$  ( $k$  is the wave number) with  $k_L < k < k_H$  ( $k_L = 2\pi/\Lambda_{\max}$ ,  $k_H = 2\pi/\Lambda_{\min}$ ). The radial profile of the magnetic field strength is  $B_r = B_0[n_e(r)/n_e(0)]^\eta$ . We set the maximum radii as  $r_{\max} = 350$  kpc, beyond which the ICMF is zero. The modified King model for the electron density distribution is assumed as in Ref. [45, 46], i.e.,  $n_e(r) = n_0(1 + r^2/r_c^2)^{-3\beta/2}$ , with parameters  $n_0 = 0.01 \text{ cm}^{-3}$ ,  $r_c = 200$  kpc,  $\beta = 2/3$ . Other parameters are given in Table I.

The extragalactic magnetic fields (EGMFs) are not clear either. The upper limit on the EGMFs given in literature is about several nG and the real value is expected to be much lower [38–42]. With  $B_T = 1$  nG, the lower criterion is about  $E_L = 2.5m_{-9}^2 g_{a\gamma,-11}^{-1} \text{ TeV}$ . The most energetic  $\gamma$ -rays of PKS 2155-304 recorded by Fermi-LAT are well below  $\sim 1$  TeV.

Therefore, we ignore the photon-ALP mixing in the EGMFs. The  $\gamma$ -rays would also be absorbed by the extragalactic background light (EBL). In this work we adopt the EBL model presented in Ref. [43].

For the magnetic fields in the Milky Way, we adopt the model developed in Ref. [35]. The Milky Way magnetic fields have both regular and striated random components. As the coherent length of the random component (100 pc or less) [36] is too short to have a significant contribution, we only take into account the regular component. The Milky Way electron density model developed in Ref. [37] is adopted.

With the information of magnetic fields, we can get the final density matrix transported from an initial pure photon beam  $\rho(s_0) = 1/2 \text{diag}(1, 1, 0)$  as

$$\rho(s) = T_{\text{MW}}T_{\text{EBL}}T_{\text{ICMF}}(s, s_0)\rho(s_0)(T_{\text{MW}}T_{\text{EBL}}T_{\text{ICMF}})^\dagger(s, s_0), \quad (15)$$

where  $T_{\text{MW}}$  and  $T_{\text{ICMF}}$  are the transfer functions in the Milky Way and the inter-cluster magnetic fields, respectively, and  $T_{\text{EBL}} = \text{diag}(e^{-\tau/2}, e^{-\tau/2}, 1)$  takes the EBL attenuation effect into account ( $\tau$  denotes the optical depth of  $\gamma$ -rays). Then the photon survival probability is given by  $P_{\gamma\gamma} = \rho(s)_{1,1} + \rho(s)_{2,2}$ .

#### IV. FERMI-LAT OBSERVATION OF PKS 2155 – 304

Our data analysis procedure is similar to that in Ref. [1]. Considering the high statistics of emission from PKS 2155 – 304, we use only the EDISP3<sup>1</sup> data to perform the analysis to achieve the best energy resolution. We follow the standard thread recommended by Fermi Collaboration<sup>2</sup> to filter the data. The SOURCE data from 2008-10-27 to 2017-06-12 (MET 246823875-518983875) for energies between 100 MeV and 500 GeV with zenith angle  $\theta_z < 90^\circ$  are selected. The selected data are binned into a count cube with  $100 \times 100$  spatial bins ( $0.1^\circ$  bin size) and 145 energy bins<sup>3</sup> to perform a binned likelihood analysis. We fitted the model to the data over the entire energy range (`global fit`) to determine the

<sup>1</sup> See [https://fermi.gsfc.nasa.gov/ssc/data/analysis/documentation/Cicerone/Cicerone\\_Data/LAT\\_DP.html](https://fermi.gsfc.nasa.gov/ssc/data/analysis/documentation/Cicerone/Cicerone_Data/LAT_DP.html) for the description of the event types in the Fermi-LAT data.

<sup>2</sup> [https://fermi.gsfc.nasa.gov/ssc/data/analysis/documentation/Cicerone/Cicerone\\_Data\\_Exploration/Data\\_preparation.html](https://fermi.gsfc.nasa.gov/ssc/data/analysis/documentation/Cicerone/Cicerone_Data_Exploration/Data_preparation.html)

<sup>3</sup> The widths of energy bins are roughly 30% of the median energy resolution of the EDISP3 data, see Ref. [1] for details.

parameters of background sources. In this step, the spectral parameters of all point sources (including the 3FGL sources and new point sources with  $\text{TS} > 25$  in the residual TS map) within a  $5^\circ$  radius are left to be free. We also left the normalizations of the two diffuse background emission components, `gll_iem_v06.fits` and `iso_P8R2_SOURCE_V6_v06.txt`, free. The background parameters were then fixed to their best-fit values in the subsequent likelihood profile analysis.

The likelihood profile in each energy bin,  $\mathcal{L}_{k'}(\mu_{k'}(P_{k'})|D_{k'})$ , is obtained by varying the prefactor  $P_{k'}$  of the target source PKS 2155–304 and calculating the corresponding likelihood  $\mathcal{L}$ . Here  $D_{k'}$  denotes the observed data in the  $k'$ -th bin, and  $\mu_{k'}$  is the expected number of photon counts which is a function of  $P_{k'}$ . As mentioned above, all background parameters are fixed in the procedure. The spectral index of PKS 2155–304 is fixed to be 2.0. We have tested that for such small energy bins, varying the index from 2.0 to 2.5 does not affect the results.

Given the photon survival probability for one ICMF realization  $B_i$ , the expected number of photon counts is

$$\mu_{k'} = \sum_k D_{kk'} \int_{\Delta E_k} dE P_{\gamma\gamma} F(E) \varepsilon(E), \quad (16)$$

where  $D_{kk'}$  is the energy dispersion which converts the theoretical numbers of photon counts in the true energy bins  $\Delta E_k$  to the expected numbers of photon counts in the reconstructed energy bins  $\Delta E_{k'}$ ,  $\varepsilon(E)$  is exposure for true energy,  $P_{\gamma\gamma}$  is the photon survival probability and  $F(E)$  is the spectrum of PKS 2155–304.

We considered three different types of spectral models for PKS 2155–304, including **Power Law**, **Broken Power Law**, and **Log-Parabola**. The log-likelihood values of the global fit for these three models are  $\log(\mathcal{L}) = -59269.9$ ,  $-59261.4$ , and  $-59260.7$ , respectively. Thus, we used the **Broken Power Law** model of PKS 2155–304 hereafter, which reads

$$F(E) = \begin{cases} NE^{-k_1}, & E < E_{\text{br}} \\ NE^{-k_2} E_{\text{br}}^{k_2-k_1}, & E \geq E_{\text{br}} \end{cases}, \quad (17)$$

where  $E_{\text{br}}$  is the break energy which is 24 GeV as obtained from the global fit.

For each ALP parameter and realization of the ICMF, we maximized the joint likelihood of all reconstructed energy bins  $\Delta E_{k'}$

$$\mathcal{L}(m_a, g_{a\gamma}, B_i, \theta|D) = \prod_{k'} \mathcal{L}(m_a, g_{a\gamma}, B_i, \theta|D_{k'}), \quad (18)$$

where  $\theta$  stands for the nuisance parameters of the intrinsic spectrum. In Fig. 1, we showed the likelihood ( $\Delta \ln \mathcal{L}$ ) map on the energy and flux plane, together with the best-fit model spectra without and with ALP (for three sets of ALP parameters).

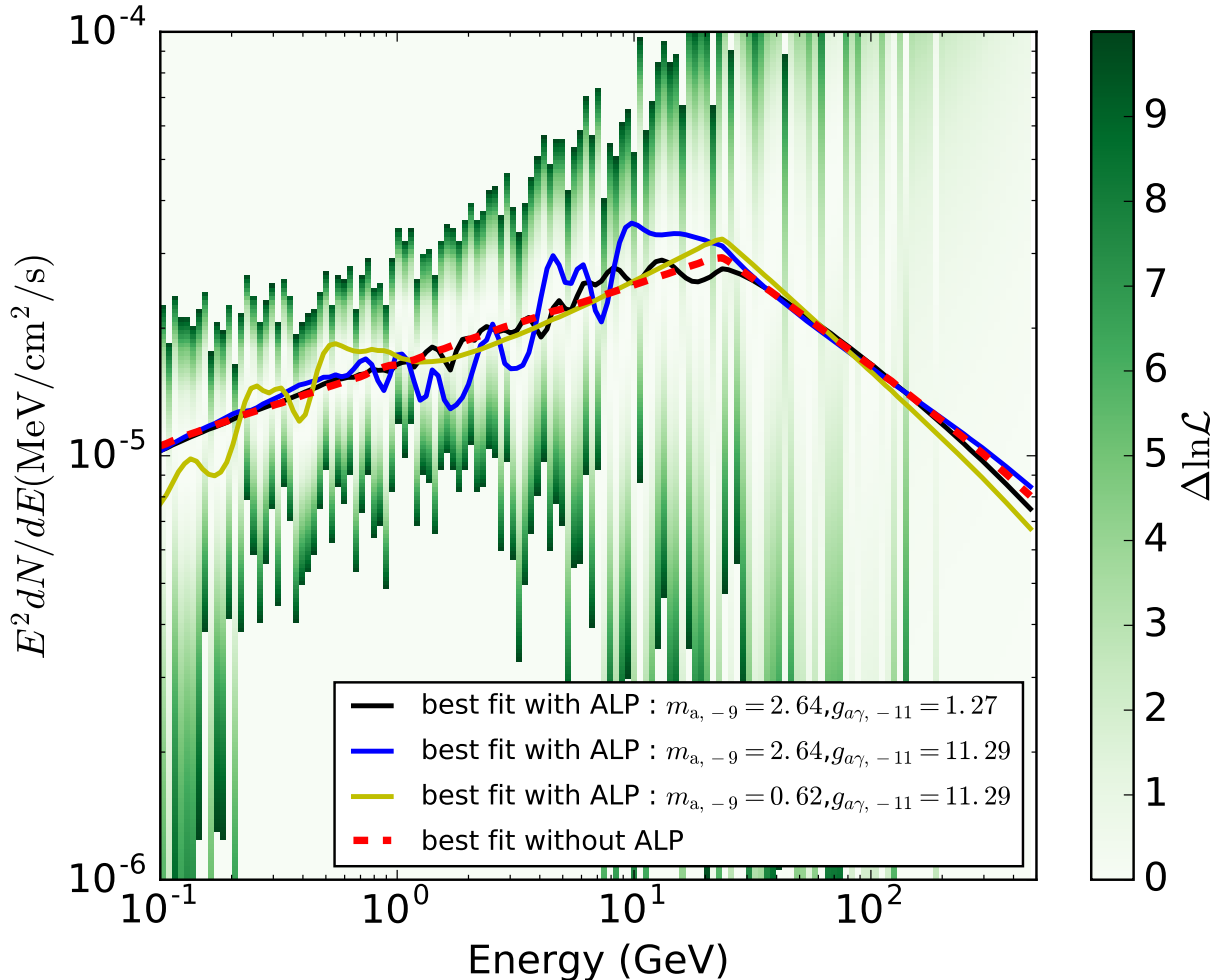


FIG. 1: Shown in color are the likelihoods,  $\Delta \ln \mathcal{L} = \ln \mathcal{L}_{\max} - \ln \mathcal{L}$ , on the plane of energy and flux. The red dashed line shows the best-fit spectrum without ALP, and the solid lines show the best-fit spectra for three sets of ALP parameters.

## V. CONSTRAINTS ON ALP PARAMETERS

It is challenging to get a well-defined likelihood of an ALP model due to the random realizations of the ICMFs. We used the Bayesian method to take the ICMF distribution into account. Flat priors of the ICMF realizations,  $\ln(m_a)$  and  $\ln(g_{a\gamma})$  are assumed. In



total, 800 realizations of the ICMFs are generated, and the prior ALP parameter ranges are  $0.1 < m_a/\text{neV} < 10^2$  and  $10^{-12} < g_{a\gamma}/\text{GeV}^{-1} < 10^{-10}$ .

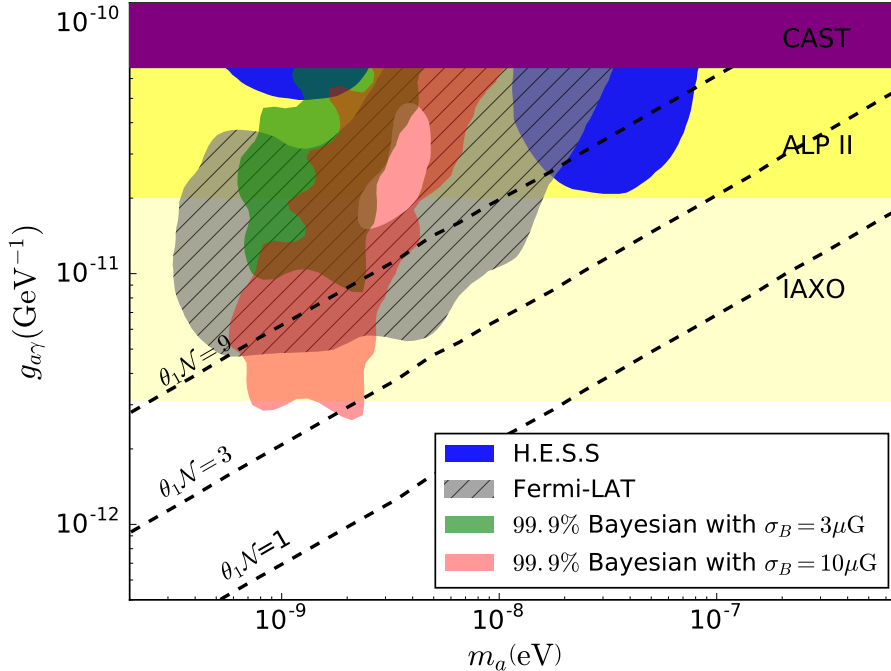


FIG. 2: Exclusion regions (red for 99% and green for 99.9% credible levels) of the ALP parameter space  $(m_a, g_{a\gamma})$  derived in this work, compared with that obtained by Fermi-LAT observation of NGC 1275 (gray; [1]) and H.E.S.S. observation of PKS 2155 – 304 (blue; [31]). The dashed line with  $\theta\mathcal{N} = 1$  ( $\theta_1\mathcal{N} = 3, \theta_1\mathcal{N} = 9$ ) denotes the parameter space that the ALP dark matter accounts for all (1/9, 1/81) of the dark matter. Some other constrains and sensitivities are adopted from [4, 20, 47–51].

The 99.9% credible level exclusion parameter regions obtained in this work are shown in Fig. 2. For comparison, we also presented the limits from previous works. With the parameters given in Table I, the exclusion region (the green one in Fig. 2.) is a strip region of  $0.6 \text{ neV} < m_a < 4 \text{ neV}$  and  $g_{a\gamma} > 10^{-11} \text{ GeV}^{-1}$ . For  $\sigma_B = 10 \mu\text{G}$ , the tightest constraint on  $g_{a\gamma}$  reaches about  $3 \times 10^{-12} \text{ GeV}^{-1}$ . In such a case, our exclusion region is comparable to (though a bit narrower than) that set by the Fermi-LAT collaboration [1] and covers the “hole”-like area. For  $\sigma_B \sim 1 - 3 \mu\text{G}$ , the constraints are weaker (see Fig. 3). Such behaviors are actually anticipated (see Sec. II). As shown in Fig. 3, the exclusion regions also depend

on  $\Lambda_{\max}$ . The other parameters do not affect the results significantly.

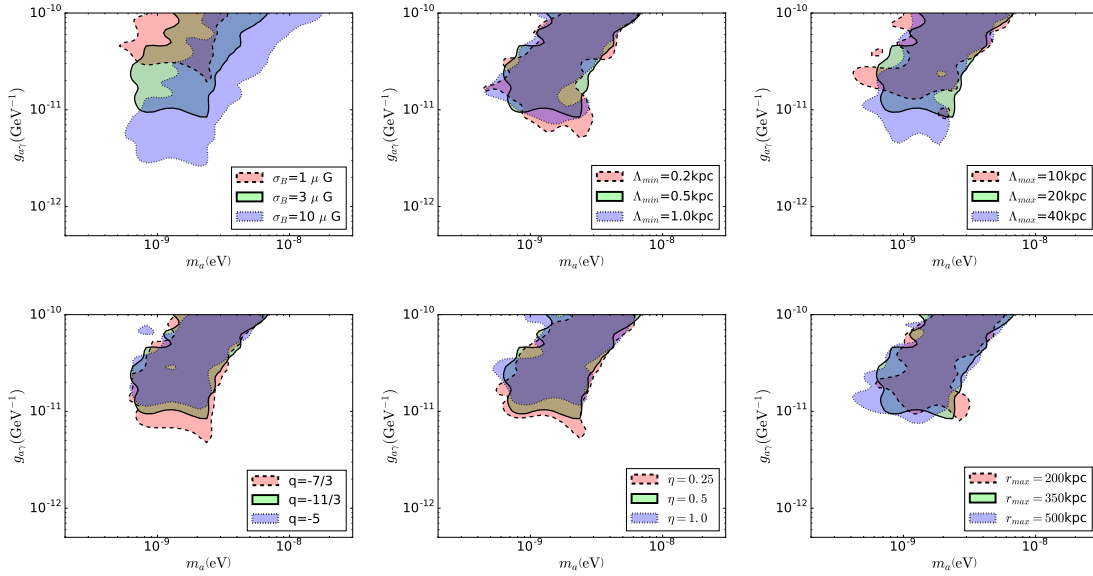


FIG. 3: The 99.9% credible level exclusion parameter regions with different ICMF parameter values. The green region with solid line is the one with the fiducial parameters given in Table I.

Future experiments such as ALP II [47] and IAXO [48] will be able to probe ALPs in a wider parameter space. As shown in Fig. 2, some reachable regions by such experiments have already been excluded by the current  $\gamma$ -ray observations. The dashed lines shown in Fig. 2 labeled as  $\theta_1\mathcal{N} = 1$ ,  $\theta_1\mathcal{N} = 3$ ,  $\theta_1\mathcal{N} = 9$  are the parameters for the ALP dark matter making up 100%, 1/9, 1/81 of the dark matter in the Universe [12]. The constraints derived in this work can exclude some of the parameter region of the ALP dark matter.

## VI. SUMMARY

The ALP-photon oscillation is caused by the direct interaction between the ALP and electromagnetic fields, which could induce spectral irregularities of high energy  $\gamma$ -ray sources due to the presence of magnetic field in the Universe. In this work, we search for such spectral irregularities in the  $\gamma$ -ray spectrum of PKS 2155 – 304 using 8.6 year Fermi-LAT observations. We do not find significant evidence for ALPs. Constraints on the parameters of ALPs are thus obtained.

We have ruled out  $g_{a\gamma} > 10^{-11} \text{ GeV}^{-1}$  for ALP mass of  $0.6 \text{ neV} < m_a < 4 \text{ neV}$  at the 99.9% credible level. If the ICMFs around PKS 2155 – 304 are as strong as  $10 \mu\text{G}$ , the

“hole”-like region allowed in previous work of Ref. [1] is excluded. As demonstrated here and in the literature, the high energy resolution observations of  $\gamma$ -ray spectra can effectively probe ALPs. The forthcoming high energy resolution data of the Dark Matter Particle Explorer [52] and the future High Energy cosmic-Radiation Detection facility [53, 54] are expected to significantly advance such studies.

### Acknowledgments

This work was supported in part by the National Key Research and Development Program of China (Nos. 2016YFA0400200 and 2016YFE0129300), the National Natural Science Foundation of China (Nos. 11535004, 11120101005, 11175085, 11773075), the Youth Innovation Promotion Association of Chinese Academy of Sciences (No. 2016288), the Natural Science Foundation of Jiangsu Province (No. BK20151608), and the Science and Technology Development Fund of Macau (No. 068/2011/A).

- 
- [1] Fermi-LAT Collaboration, *Phys. Rev. Lett.* **116** 161101 (2016).
  - [2] R. D. Peccei and H. R. Quinn, *Phys. Rev. Lett.* **38**, 1440 (1977); R. D. Peccei and H. R. Quinn, *Phys. Rev. D* **16**, 1791 (1977).
  - [3] J. H. Kim, *Phys. Rep.* **150**, 1 (1987).
  - [4] J. E. Kim and G. Carosi, *Rev. Mod. Phys.* **82**, 557 (2010).
  - [5] S. Weinberg, *Phys. Rev. Lett.* **40**, 223 (1978); F. Wilczek, *Phys. Rev. Lett.* **40**, 279 (1978).
  - [6] M. B. Wise, H. Georgi, and S. L. Glashow, *Phys. Rev. Lett.* **47**, 402 (1981).
  - [7] P. Svrcek, E. Witten, *JHEP* **0606**, 051 (2006).
  - [8] S. B. Giddings and A Strominger, *Nucl. Phys. B* **306**, 890 (1998).
  - [9] L. DiLella, A. Pilaftsis, G. Raffelt, K. Zioutas *Phys. Rev. D* **62**, 125011 (2000).
  - [10] S. Chang, S. Tazawa and M. Yamaguchi, *Phys. Rev. D* **61**, 084005 (2000).
  - [11] N. Turok, *Phys. Rev. Lett.* **76**, 1015 (1996).
  - [12] P. Arias, D. Cadamuro, M. Goodsell, J. Jaeckel, J. Redondo, and A. Ringwald, *J. Cosmol. Astropart. Phys.* **6**, 013 (2012).
  - [13] P. Arias, J. Jaeckel, J. Redondo, and A. Ringwald, *Phys. Rev. D* **82**, 115018 (2010).

- [14] A. Ringwald, Phys. Dark Univ. **1**, 116 (2012).
- [15] B. W. Lee and S. Weinberg, Phys. Rev. Lett. **39**, 165 (1977).
- [16] J. E. Gunn, B. W. Lee, I. Lerche, D. N. Schramm, and G. Steigman, ApJ **223**, 1015 (1978).
- [17] Z. Ahmed *et al.* (CDMS), Science **327**, 1619 (2010).
- [18] E. Aprile *et al.* (XENON100 Collaboration), Phys. Rev. Lett. **109**, 181301 (2012).
- [19] G. Ambrosi, et al. (DAMPE collaboration), Nature, **552**, 63 (2017).
- [20] S. Andriamonje, *et al.*, J. Cosmol. Astropart. Phys. **0704** 010 (2007).
- [21] K. Zioutas, *et al.*, Phys. Rev. Lett. **94** 121301 (2005).
- [22] V. Anastassopoulos *et al.*, Nature Physics **13**, 584 (2017).
- [23] K. Ehret, M. Frede, S. Ghazaryan, M. Hildebrandt, E. A. Knabbe, *et al.*, Phys.Lett. B **689**, 149 (2010).
- [24] M. Betz, F. Caspers, M. Gasior, M. Thumm, and S. W. Rieger Phys. Rev. D **88**, 075014 2013.
- [25] P. W. Graham and S. Rajendran Phys. Rev. D **88**, 035023 (2013).
- [26] L. J. Rosenberg and K. A. van Bibber, Phys. Rept. **325**, 1 (2000).
- [27] R. Bradley *et al.*, Rev. Mod. Phys. **75**, 777 (2003).
- [28] P. Graham, I. Irastorza, S. Lamoreaux, A. Lindner, and K. van Bibber Ann. Rev. Nucl. Part. Sci. **65** 485 (2015).
- [29] J.C. Wheeler, I. Yi, P Höflich and L Wang Astrophys. J. **521**, 179 (1999).
- [30] D. Chelouche, R. Rabadán, S. S. Pavlov and F. Castejón, Astrophys. J. Suppl. **180**, 1 (2009).
- [31] A. Abamoski *et al.* H.E.S.S Collaboration Phys. Rev. D **88** 102003 (2013).
- [32] G.Raffelt and L. Stodolsky Phys. Rev. D **37**, 1237 (1988).
- [33] W. Heisenberg and H. Euler, Z. Phys. **98**, 714 (1936).
- [34] C. M. Urry and R. F. Mushotzky , Astrophys. J. **253** 38(1982).
- [35] J. Ronnie and F. R. Glenny, Astrophys. J. **757** 14 (2012).
- [36] M. Haverkorn, J. C. Brown, B. M. Gaensler, and N. M. McClure-Griffiths, Astrophys. J. **680**, 362 (2008).
- [37] M. J. Cordes, T. Lazio and W. Joseph, arXiv: astro-ph/0207156 (2002).
- [38] M. S. Pshirkov, P. G. Tinyakov and F. R Urban, Phys. Rev. Lett. **116** 191302 (2016).
- [39] P. P. Kronberg,, Rept.Prog.Phys. **57**, 325 (1994).
- [40] Planck Collaboration, P. A. R. Ade, N. Aghanim, M. Arnaud, F. Arroja, M. Ashdown, J. Aumont, C. Baccigalupi, M. Ballardini, A. J. Banday, and et al., arXiv:1502.01594 (2015).

- [41] J. D. Barrow, P. G. Ferreira, and J. Silk, *Phys.Rev.Lett.* **78**, 3610 (1997).
- [42] Y. Z. Fan, Z. G. Dai, and D. M. Wei, *Astron. Astrophys.* **415**, 483 (2004).
- [43] A. Franceschini, G. Rodighiero and M. Vaccari, *Astron. Astrophys.* **487**, 837 (2008).
- [44] M. Meyer and D. Montanino and J. Conrad, *JCAP* **9** 003 (2012).
- [45] C.L. Carilli, G.B. Taylor *Ann. Rev. Astron. Astrophys.* **40**, 319 (2002).
- [46] A. Cavaliere, R. Fusco-Femiano *Astron. Astrophys.* **49**, 137 (1976).
- [47] R Bähre et al., *JINST* **8**, T09001 1302.5647 (2013).
- [48] I.G. Irastorza , et al. *J. Cosmol. Astropart. Phys.* **6** 013 (2011).
- [49] V. Anastassopoulos et al., *Nature Physics* **13**, 584 (2017).
- [50] M. Meyer and J. Conrad, *J. Cosmol. Astropart. Phys.* **12**, 016 (2014).
- [51] J. L. Hewett *et al.*, arXiv:1205.2671 (2012).
- [52] J. Chang, et al. (DAMPE collaboration), *Astropart. Phys.* **95**, 6 (2017).
- [53] S. N. Zhang et al. (HERD Collaboration), *Proc. SPIE Int. Soc. Opt. Eng.* **9144**, 91440X (2014).
- [54] X. Huang *et al.*, *Astropart. Phys.* **78**, 35 (2016).